Available online at www.sciencedirect.com
SCIENCE DIRECT®
Journal of Hydrology 311 (2005) 172–187
Journal of Hydrology
www.elsevier.com/locate/jhydrol

Rainfall erosivity and variability in the Northern Ethiopian Highlands

J. Nyssen[a,b,*], H. Vandenreyken[a], J. Poesen[a], J. Moeyersons[c], J. Deckers[d], Mitiku Haile[b], C. Salles[a,e], G. Govers[a]

[a]*Physical and Regional Geography Research Group, Katholieke Universiteit Leuven, Redingenstraat 16, B-3000 Leuven, Belgium*
[b]*Department of Land Resources Management and Environmental Protection, Mekelle University, P.O. Box 231, Mekelle, Ethiopia*
[c]*Royal Museum for Central Africa, B-3080 Tervuren, Belgium*
[d]*Institute for Land and Water Management, K.U. Leuven, Vital Decosterstraat 102, B-3000 Leuven, Belgium*
[e]*Laboratoire HydroSciences Montpellier (UMR 5569), Université Montpellier II, Case Courrier MSE, F-34095 Montpellier Cédex 5, France*

Received 17 May 2004; revised 20 December 2004; accepted 21 December 2004

Abstract

The Ethiopian Highlands are subjected to important land degradation. Though spatial variability of rain depth is important, even at the catchment scale, this variability has never been studied. In addition, little is known on rain erosivity for this part of the world. The objectives of this study are (a) to assess the spatial variation of rain in a 80 km^2 mountain area (2100–2800 m a.s.l.) in the Northern Tigray region, and how this variation is influenced by topography, geographical position and lithology, (b) to analyse the temporal variations and (c) to quantify rain erosivity and the different factors determining it, such as rain intensity, drop size and kinetic energy.

Spatial variation of rain was measured over a 6-y period by installing 16 rain gauges in the study area. Topographical factors, especially general orientation of the valley and slope gradient over longer distances, determine the spatial distribution of annual rain, which is in the order of 700 mm y^{-1}. Precipitation is highest nearby cliffs and other eminent slopes, perpendicular to the main valleys which are preferred flow paths for the air masses.

Rain intensity is smaller than expected: 88% falls with an intensity <30 mm h^{-1}. High intensities have a short duration; maximum recorded rain depth over 1 h (32 mm) is only 2 mm less than that over 24 h. Using the blotting paper method 65,100 rain drops were sampled. For all observed rain intensities, the median volume drop diameters (D_{50}) are significantly larger than those reported for other regions of the world. A relation between rain intensity (I) and volume specific kinetic energy (Ek_{vol}) was developed for the Ethiopian Highlands:

$$Ek_{vol} = 36.65(1 - (0.6/I)) \quad (R^2 = 0.99,\ n = 18),\ (Ek_{vol} \text{ in J m}^{-2}\text{ mm}^{-1},\ I \text{ in mm h}^{-1}).$$

Due to the occurrence of large drop sizes, probably linked to the prevailing semi-arid to subhumid mountain climate, this relation yields, within the intensity range [0.6–84 mm h^{-1}], larger values for Ek_{vol} than elsewhere in the world.

* Corresponding author. Address: Institute for Land and Water Management, Katholieke Universiteit Leuven, B-3000 Leuven, Belgium.
E-mail address: jan.nyssen@agr.kuleuven.ac.be (J. Nyssen).

0022-1694/$ - see front matter
doi:10.1016/j.jhydrol.2004.12.016

It is recommended to use this new relationship for calculating Ek_{vol} of rain in the Ethiopian Highlands, as well as for the computation of Universal Soil Loss Equation's rain erosivity factor on yearly basis.

Keywords: Rain; Spatial variation; Intensity; Erosivity; Rain drop size; Rain kinetic energy; Ethiopia

1. Introduction

Besides its importance for agriculture, precipitation is the driving force of most water erosion processes, through detachment of soil particles and creation of surface runoff (Moore, 1979). Rain is also a triggering factor for mass movements.

Due to the presence of numerous topographic obstacles for dominant winds, orographic rain is common in many parts of Ethiopia, especially in the Rift Valley. However, convective movements of air masses, caused by differential heating of the earth surface, and resulting rains of high intensity and often short in duration are most widespread in Ethiopia (Krauer, 1988).

There are various rain regimes in the different regions of Ethiopia. Attempts to regionalise rain patterns were made by Suzuki (1967), Troll (1970), Daniel (1977) and Goebel and Odenyo (1984). The variability of rain patterns also results in yearly rain depths being almost independent from elevation, at country scale (Krauer, 1988). Above 1500 m a.s.l., other factors, including slope aspect and characteristics of dominant air masses, mask the possible relationship between elevation and mean yearly rain. Eklundh and Pilesjö (1990) regionalised the explanatory factors of rain depth, using principal component analysis. Results show that in most regions elevation is not an explanatory factor. Unlike elsewhere (e.g. Marquinez et al., 2003), no in-depth studies of explanatory factors of rain distribution have ever been conducted at local scale in Ethiopia, though this is of utmost importance for predictions of crop productivity and rates of land degradation processes.

Rain erosivity is a function of the rain's physical characteristics. In tropical regions rains are intense. These characteristics, as well as rain depth, drop size distribution, terminal fall velocity, wind speed and rain inclination, determine rain erosivity (Obi and Salako, 1995). Raindrop sizes have been measured and analysed in many countries. However, to our knowledge, in Africa such studies only exist for Zimbabwe (Hudson, 1965; Kinnell, 1981) and Nigeria (Kowal and Kassam, 1976; Aina et al., 1977; Lal, 1998). Drop size distribution, for a given intensity, is unimodal and slightly skewed to the left (Brandt, 1990). Often, a relationship of the type

$$D_{50} = aI^b \tag{1}$$

is expected between the median volume drop diameter (D_{50}) and rain intensity (I), with a and b being constants for a given region (Hudson, 1971). This type of relationship is however questioned for high intensities, since raindrops have a maximum size (Hudson, 1971).

The calculation of volume specific kinetic energy of a raindrop

$$Ek_{vol} = (mv^2)/2 \tag{2}$$

involves transformation of average drop diameter into mass (m), assuming that raindrops are spherical, and an assessment of the terminal fall velocity (v) of raindrops of different sizes, as experimentally obtained by Laws (1941). Calculations of kinetic energy generally show that there is an increase up to an intensity of about 75 mm h^{-1}, above which Ek_{vol} remains constant (Wischmeier and Smith, 1958; Hudson, 1971; Jayawardena and Rezaur, 2000; Salles et al., 2002). Measurements of kinetic energy and raindrop sizes are in most cases not readily available; hence the development of empirical relationships between rain intensity and kinetic energy, which is in general expressed on a volume-specific basis, in J m^{-2} mm^{-1}. Time-specific kinetic energy (Ek_{time}), which is related to Ek_{vol} by

$$Ek_{time} = Ek_{vol}I \quad (\text{in J m}^{-2}\ \text{h}^{-1}) \tag{3}$$

gives generally better correlations with rain intensity (Salles et al., 2002).

A recent literature review (Van Dijk et al., 2002) learns that most studies relating rain erosivity to drop size were carried out in regions located at a maximum

of a few hundred metre a.s.l., with some rare exceptions reaching 2250 m a.s.l. (Blanchard, 1953). Consequences of lesser fall height for rain drop size in mountain areas are hence not taken into account.

In Ethiopia, calculations of erosivity parameters rely entirely on $I-\mathrm{Ek}_{\mathrm{vol}}$ relations established in other parts of the world, and especially on the Wischmeier and Smith (1958) equation based on data from a few stations in North America (Van Dijk et al., 2002). Renard et al. (1997) no longer recommend that equation.

The objectives of this study are to investigate (a) the spatial variation of rain in the study area, and how this is influenced by elevation, slope aspect and gradient, as well as geographical position; (b) the temporal variations of rain; and (c) rain erosivity in terms of the different controlling parameters, such as rain intensity, rain drop size and kinetic energy.

2. Materials and methods

2.1. The study area in the Northern Ethiopian Highlands

The climate of Ethiopia is complex: 'Within short horizontal distances, climates from tropical to sub-humid, and subtropical to arctic can occur' (Krauer, 1988). For a given altitudinal level precipitation decreases and seasonality increases with latitude.

During the winter in the Northern hemisphere, the Intertropical Convergence Zone (ITCZ) is situated to the South of the equator in Eastern Africa. At this time of the year, the western Highlands of Ethiopia receive hot and very dry winds from the Sahara. On the other hand, the Red Sea coast and the eastern part of the country are under the influence of east winds, with a high moisture content after their journey over the Indian Ocean. These winds also bring spring rains in the southern part of Ethiopia. From March till May, rains accompany the movement to the North of the ITCZ and the equatorial air masses. These rains are triggered by the convergence of humid equatorial air and colder extratropical air (Suzuki, 1967; Troll, 1970; Daniel, 1977; Messerli and Rognon, 1980; Goebel and Odenyo, 1984).

From the end of June onwards, the ITCZ is situated at its most northerly position (16–20°N). The south–east monsoons, limited to the lower layers of the atmosphere, bypass the Highlands by the South and reach them from the West, provoking the rainy season (Goebel and Odenyo, 1984). Other authors attribute the origin of these humid air masses, coming from the West, to the Atlantic Ocean. They would pass over the equatorial forest where vapour is taken in (Hemming, 1961; Suzuki, 1967; Daniel, 1977; Rudloff, 1981). Generally, clouds are formed at the end of the morning, as a result of evaporation and convective cloud formation due to daytime heating of the land, and it rains in the afternoon. In Afdeyu station, on the Eritrean Highlands, 80% of daily precipitation takes place between 12 and 16 h (Krauer, 1988). Slopes exposed to the West, to the afternoon sun, receive less sunshine. This convective nature of rain also explains why individual showers have a very local distribution.

At the end of the summer, the ITCZ returns quickly to the South, preventing the arrival of monsoons. This is the end of the rainy season in the Highlands.

Abebe and Apparao (1989) calculated a mean annual precipitation of 938 ($\pm$83) mm y^{-1} from 241 stations in Ethiopia. In the highlands, average annual rain varies between 600 mm y^{-1} in Tigray and more than 2000 mm y^{-1} in the south-western Highlands (Krauer, 1988).

The Dogu'a Tembien district (Fig. 1), located in Tigray, on the rift shoulder at the west of the Danakil depression, was selected as research area for this study, since its elevation and morphology are typical for the Northern Ethiopian Highlands. The Atbara-Takazze river system drains the water of the study area to the Nile. The district is situated some 50 km W of Mekelle, regional capital of Tigray.

Hagere Selam, the main town of the district, is located at an elevation of 2650 m a.s.l., on the road Mekelle-Adwa. The geomorphology of the study area is strongly controlled by the subhorizontal structure of the lithology and by rapid incision (Mohr, 1963; Merla et al., 1973). The presence of faults and lineaments (lines of weakness) influences the pattern of the river systems. The uplift being recent, the rivers are in their juvenile stadium, and deeply incised.

Except for some dykes, all geological formations in the study area (Arkin et al., 1971; Beyth, 1972) contribute to the formation of a stepped morphology: (1) the Mesozoic sedimentary layers (Hutchinson and Engels, 1970) are subhorizontal and present

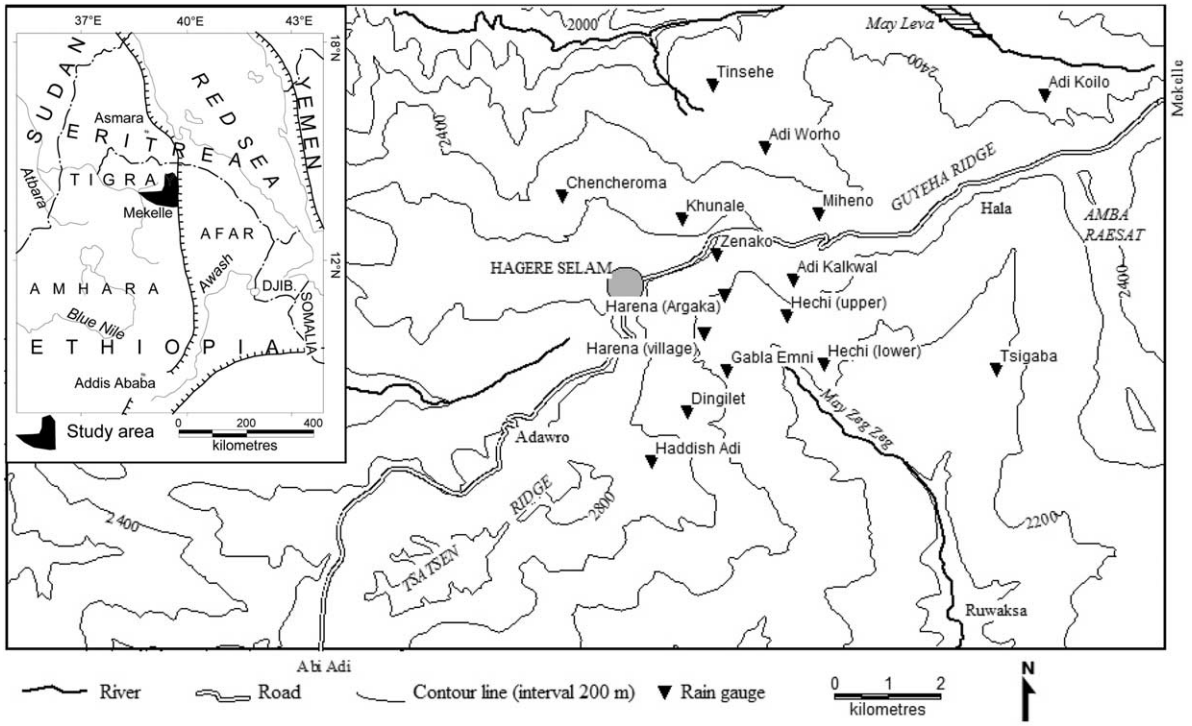

Fig. 1. Map of the study area with location of the rain gauges.

alternating hard and soft layers; (2) the basalt flows (Garland, 1980) are subhorizontal and interbedded with soft silicified lake deposits; (3) sills of Mekelle dolerite also form hard, subhorizontal layers. The relief thus consists of an alternation of flats and escarpments, expressing the unequal resistance of the rocks subjected to weathering. The edges of these scarps are nearly horizontal, underlining the tabular structure.

Due to the mountainous character of the district and to poverty-induced extensive agriculture, many soil erosion problems are encountered. At present, they are tempered by an active soil conservation policy (Nyssen et al., 2000, 2004).

2.2. Rain gauge network

Sixteen rain gauges were installed at various locations in the study area, on a total area of approximately 80 km^2 (Fig. 1). The rain gauges were constructed with simple materials: a cylinder made from two metal tins was fixed in cement, on top of a 1.5 m high tower. A strong plastic bottle, with a funnel fixed at its top was inserted in the tins (Fig. 2). Orifices of the funnels were horizontal.

The rain gauges were more or less evenly spread over the study area. They were located near houses for supervision; this location resulted sometimes in

Fig. 2. Cross-section of rain gauge (Harena-Argaka). Note the two metal tins fixed in cement (arrows), which hold a plastic bottle with funnel (diameter = 12.7 cm).

Fig. 3. A typical location for a rain gauge: on a fence near a house (Haddish Addi).

obstacles (especially eucalyptus trees) that needed to be regularly removed from their vicinity. For most rain gauges, these obstacles were at the minimal distance (twice the height of the obstacle), recommended by some meteorological services (Houghton, 1985); the distance was always larger than the height of the tree itself. Sometimes rain gauges were installed on rooftops, to avoid such obstacles. Due to the nature of the terrain, the rain gauge locations were generally inclined (Fig. 3), which is also not recommended, but which allowed introducing slope aspect in the analysis. Rain gauges were read daily by secondary school students residing in the neighbourhood; the volume of water in the bottle was determined using a measuring gauge. Quality control of the data and checks of the precision of the readings showed that errors were very small. Observations covered 6 y (1998–2003) for 9 rain gauges, 4 y for three others and 2 y for the whole set of 16 gauges including the previously mentioned (Table 1).

For all sites, possible explanatory variables for rainfall distribution were recorded (Table 1). A reformulation of hypotheses of rain distribution was done after a preliminary analysis of data covering 4 y (1998–2001) (Vandenreyken et al., 2001); this involved the expansion of the rain gauge network. Possible explanatory variables included:

- Geographical position, expressed in UTM coordinates, the axes of which, in the study area, correspond perfectly to W–E and S–N directions; in addition, coordinates along NW–SE and SW–NE axes were calculated
- Elevation
- Local slope aspect (A_{local})
- Aspect of the main valley in which the station was located (A_{valley})
- Parameters describing topographic effects: for each rain gauge, the nearest point with a vertical interval of 50 m upslope and 200 viz. 500 m downslope were determined from topographic maps (Ethiopian Mapping Authority, 1996) and the slope gradient between the station and these points calculated (S_{50up}, $S_{200down}$, $S_{500down}$)
- The distance to limestone areas, expected to be less favourable to convective rain, was expressed as the distance to the centre of the nearest contiguous area (of 1 and 5 km^2) with limestone parent material, using a geological map (Arkin et al., 1971); evidently, for stations well within the limestone zone, this distance is 0 (LIM_1 and LIM_5)

One tipping bucket rain gauge with a precision of 0.2 mm was installed in March 1998. Minute-based measurements were recorded by datalogger. The data obtained were used to characterise rain intensity in the study area.

Table 1
Characteristics of the rain gauge stations

Rain station	X coordinates (UTM, m)	Y coordinates (UTM, m)	Coordinates along X' (NW–SE, m)	Coordinates along Y' (SW–NE, m)	Elevation (m a.s.l.)	A_{local} (deg)[a]	A_{valley} (deg)[a]	LIM_1 (km)	LIM_5 (km)	S_{50up} (m m^{-1})	$S_{200down}$ (m m^{-1})	$S_{500down}$ (m m^{-1})	n
Hechi (lower)	522,313	1,507,376	−696,544	1,435,206	2275	228	139	0	0	0.061	0.109	0.045	6
Hechi (upper)	521,603	1,508,279	−697,685	1,435,342	2330	194	139	0	0	0.199	0.162	0.052	6
Adi Kalkwal	521,719	1,508,945	−698,074	1,435,895	2470	166	133	0.223	0.467	0.102	0.256	0.113	6
Zenako	520,289	1,509,434	−699,431	1,435,230	2540	150	139	0.565	1.551	0.327	0.296	0.114	6
Harena (Argaka)	520,434	1,508,661	−698,782	1,434,786	2350	173	139	0	1.114	0.331	0.123	0.059	6
Harena (village)	520,052	1,507,941	−698,543	1,434,007	2390	74	114	0.945	1.593	0.137	0.121	0.059	6
Gabla Emni	520,479	1,507,234	−697,741	1,433,809	2400	26	139	1.151	1.693	0.117	0.186	0.069	6
Dingilet	519,723	1,506,467	−697,733	1,432,732	2530	103	89	1.984	2.954	0.106	0.225	0.137	6
Haddish Adi	519,050	1,505,530	−697,546	1,431,593	2730	42	37	2.812	3.244	0.115	0.178	0.204	6
Khunale	519,648	1,510,092	−700,349	1,435,242	2560	340	0	1.291	2.461	0.229	0.134	0.159	4
Adi Worho	521,189	1,511,450	−700,220	1,437,292	2460	350	327	0.43	0.749	0.161	0.077	0.054	4
Miheno	522,197	1,510,188	−698,615	1,437,112	2520	39	327	1.402	1.798	0.157	0.087	0.091	4
Chencheroma	517,392	1,510,528	−702,253	1,433,955	2517	290	5	1.916	2.523	0.088	0.248	0.252	2
Tsigaba	525,558	1,507,269	−694,174	1,437,425	2093	286	200	0	0	0.199	0.044	0.037	2
Tinsehe	520,216	1,512,629	−701,741	1,437,438	2293	1	263	0	0	0.175	0.170	0.051	2
Adi Koilo	526,470	1,512,437	−697,183	1,441,724	2386	219	297	0.183	1.039	0.086	0.033	0.038	2

A_{local}, local slope aspect; A_{valley}, general aspect of the main valley; LIM_1: distance to centre of nearest contiguous limestone area of 1 km^2; LIM_5, distance to centre of nearest contiguous limestone area of 5 km^2; S_{50up}, slope gradient over a vertical interval of 50 m upslope from the rain gauge; $S_{200down}$, slope gradient over a vertical interval of 200 m downslope from the rain gauge; $S_{500down}$, slope gradient over a vertical interval of 500 m downslope from the rain gauge; n, number of years of observation.

[a] Turning right from the N.

2.3. Raindrop size measurements

Raindrop sizes were measured in July–September 2000 in Hagere Selam (see Fig. 1) using the blotting paper method (Hall, 1970; Poesen, 1983). Other methods, such as the optical spectro pluviometer (Salles and Poesen, 1999), though less time consuming, could not be used for logistic reasons. Blotting paper (280 g m^{-2}) was cut into sheets of 9 cm × 15 cm. During rain events, these sheets were exposed to the rain until the stains started overlapping. During the transfer period from inside the house to the measuring place, and back to the house again, the sheets of blotting paper were covered by a tray. Time was registered on the sheet and stains were immediately outlined by pencil by a team of 3–5 people working inside.

The underlying principle for this method is that a drop falling on a uniformly absorbing surface creates a stain with a diameter proportional to the drop diameter. Poesen (1983) established a calibration curve for stains 0.6–6 mm on blotting paper of 280 g m^{-2}:

$$\varnothing_{st} = 2.44\varnothing_{dr} \quad (r^2 = 0.99;\ n = 9) \tag{4}$$

where

$\varnothing_{st}$ diameter of stain on blotting paper (mm)
$\varnothing_{dr}$ diameter of water drop (mm).

This calibration equation was tested with the blotting paper we used in the experiment. Measurement of the stain diameters was carried out with a precision of 0.25 mm. In case of elongated stains, these were considered to be the result of a coalescence of two stains, and measured as such. In total, 65,100 raindrops were outlined and measured (Vandenreyken, 2001).

The tipping bucket rain gauge was operating at a few metres distance from the place where the drop-size measurements were done, which allowed linking rain intensity to corresponding measurements of raindrop sizes. One tip of the tipping bucket rain gauge (resolution: 1 min) corresponds to an intensity of 12 mm h^{-1}. Time spans >1 min between two successive tips were only taken into account if there was continuous rain; here, intensity was calculated by dividing 12 mm h^{-1} by the number of minutes between two successive tips. Measurements at the beginning and the end of a shower, when the bucket in the gauge did not tip, as well as measurements carried out at a moment when there was a rapid variation in rain intensity, were discarded. Furthermore, there is no bias towards the measurement of large drops in this methodology, because (1) drop sampling was stopped as soon as stains started overlapping, and (2) the volume of a few possible missed small drops would be negligible.

2.4. Statistical methods

The degree of association between variables was measured by regression and calculation of the Pearson correlation coefficient r. The significance of these coefficients was tested at different probability levels (P) by F-tests (Beguin, 1979).

Rain distribution was modelled by non-linear multiple regressions; stepwise models were created, at each step leaving out the least significant explanatory variable. The interpretation of the variables involved the determination of the functional relationship between the dependent and independent variables.

3. Results and discussion

3.1. Temporal variation of rain

3.1.1. Daily rain

Over three rainy seasons, the tipping bucket rain gauge recorded 204 rain events (taking into account that the gauge did not function during 1 month) of 15 min of duration at least and were separated by 30 min at least. These 204 events were classified by the time (hour) of their start (Table 2). Forty seven percent of the events start in the afternoon and 30% in the evening (18–24 h), providing 84% of total rain. It hardly ever rains much before noon. This daily rain pattern is explained by the dominance of convective rains, caused by the heating of the earth's surface during the morning (Krauer, 1988). Griffiths (1978) states that rain during the night is preferable for agriculture since there is less evaporation. While this is certainly true in areas and periods with moisture

Table 2
Classification of rain events by their corresponding moment of initiation during the day

Begin of rain event (time, h)	Number of events	Relative number of events (%)	Average duration of event (min)	Average rain depth for one event (mm)	Rain depth (mm)	Proportion of total rain (%)
0–6 AM	35	17	99	4.6	162	12
6–12 AM	13	6	76	3.7	48	4
12–18 PM	95	47	66	7.5	718	55
18–24 PM	61	30	70	6.3	382	29

stress, this might not be so in some parts of the study area having saturated clay soils in August.

3.1.2. Annual rain

Dry and rainy seasons are clearly visible on the diagrams indicating mean monthly rain for all stations. As an example, the Dingilet rain diagramme (Fig. 4) gives a clear illustration of the unimodal rain pattern. It should be stressed that, if on average there is some rain between October and May, it is highly unreliable (see magnitude of standard deviations).

The precipitation coefficient, i.e. the average monthly precipitation divided by one-twelfth of the average yearly precipitation allows characterising the different months (Daniel, 1977). October to May are dry months (coeff. <0.6), June and September have coefficients (1.0–1.9). A very high concentration of rain is observed in July and August (coeff. >3.0). Remarkably, there are no months with intermediate precipitation coefficients (2.0–3.0).

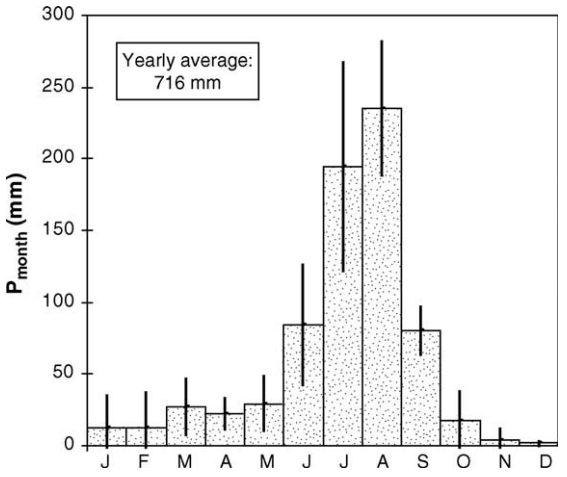

Fig. 4. Mean (1998–2003) monthly rain (P_{month}) in Dingilet, shown with one standard deviation.

3.1.3. Interannual rain variability

As shown in Fig. 5, interannual rain variability is also very important. Average yearly rainfall depth (nine stations) in the study area ranged between 546 mm in 2002 and 879 mm in 1998. In semi-arid to subhumid areas, such rain variability and unpredictability has important consequences for agricultural production. However, based on our short 6 y data series, nothing can be said with regard to long-term tendencies.

A literature review of interannual variability in precipitation in the Ethiopian Highlands shows that analyses of time series till 1990 give contradictory results. For Yilma and Demarée (1995), 'a decline of the rainfall in the Sahel observed since about 1965 is also seen on a lesser scale in the north central Ethiopian Highlands'. Camberlin (1994) found a similar tendency. However, unlike the Sahel, a comparison between two reference periods (1931–1960 and 1961–1990) yields no significant changes in mean rain over Ethiopia, but an increased interannual variability (Hulme, 1990). Mattson and Rapp (1991) state that 'it is not clear whether this pattern signifies the beginning of a long-term reduction or is within the range of normal

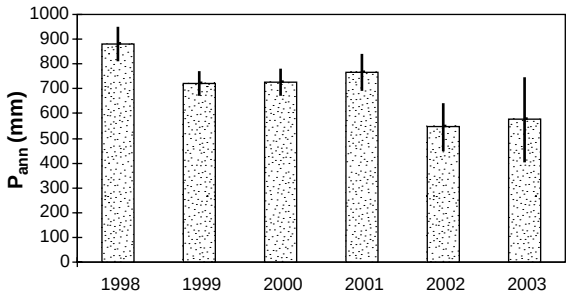

Fig. 5. Mean (nine stations) annual rain (P_{ann}) for the period 1998–2003 in Dogu'a Tembien. The standard deviation indicates the variability between the different rainfall stations.

fluctuations'. Analyses of time series of annual precipitation, reaching up to 2000 AD, both for Addis Ababa and the Northern Highlands, show that although the succession of dry years between the late 1970s and late 1980s produced the driest decade of the previous century in the Ethiopian Highlands, there is no evidence for a long-term trend or change in the region's annual rain regime (Conway, 2000; Nyssen et al., 2004).

3.2. Spatial variation of rain

Observed mean (6 y) measured annual rain depth in the study area varies between 631 and 718 mm y^{-1} (Table 1). Between the highest and the lowest rain gauge, there is a difference in elevation of 637 m. However, statistical analysis shows that the correlation between elevation and yearly rain is not significant (Table 4). Correlation coefficients for individual years are even smaller. It was checked if this weak correlation might be due to the occurrence of local, convective rains. Days with large differences in rain depth between the stations were estimated to be convective and not taken into account in the analysis; this did not improve the correlation. Hence, elevation is not the major factor determining yearly rain in the study area, confirming, for a rather small area, the observations made by Krauer (1988) for the whole country (Fig. 6).

Analysis of data in Table 3 shows that there is a good correlation between the 6 y average annual rainfalls and the 4 or 2 y average annual rainfalls (r^2 ranging between 0.64 and 0.85). This indicates that the relative differences in rainfall between rain gauges are determined by one or more features related to their geographical or topographical situation. Visual observations in the study area show that intense rains, rather of the convective type, are often first observed at lower altitudes, from where they move upslope through valleys. Stations (partly) at the leeward side receive less precipitation. Variables that could possibly explain the path of such intense showers can be (1) preferred flow paths for air masses through large valleys during the rainy season, (2) the presence of a limestone–basalt lithological limit; the lower albedo of the dark basalt-derived materials would create more rapid warming up and stronger convective movements as compared to limestone areas, and (3) a topographic effect. All these variables were

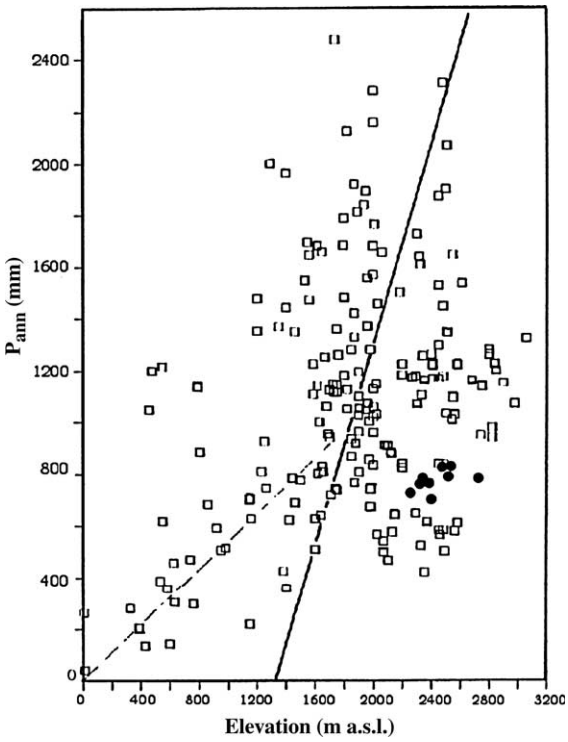

Fig. 6. Mean annual rain depth (P_{ann}) vs. elevation for Ethiopia ($r^2=0.12$). Squares after Krauer (1988). Circles correspond to results from this study in Dogu'a Tembien.

Table 3
Average yearly rainfall (mm y^{-1}) for 12 gauges in Dogu'a Tembien1

	1998–2003 (6 y)	2000–2003 (4 y)	2002–2003 (2 y)
Hechi (lower)	679	651	542
Hechi (upper)	718	679	575
Adi Kalkwal	707	624	540
Zenako	681	575	471
Harena (Argaka)	708	659	540
Harena (village)	705	667	562
Gabla Emni	631	574	463
Dingilet	716	682	538
Haddish Adi	706	663	544
Khunale		645	628
Adi Worho		632	564
Miheno		668	562
Chencheroma			940
Tsigaba			599
Tinsehe			446
Adi Koilo			459

Table 4
Coefficients of determination (r^2) for the relations between annual rain depth corresponding to the stations and different explanatory factors

Coefficient of determination, r^2	X coordinates (UTM, m)	Y coordinates (UTM, m)	Coordinates along X' (NW–SE, m)	Coordinates along Y' (SW–NE, m)	Elevation (m a.s.l.)	A_{local} (deg)[a]	A_{valley} (deg)[a]	LIM_1 (km)	LIM_5 (km)	S_{50up} (m m^{-1})	$S_{200down}$ (m m^{-1})	$S_{500down}$ (m m^{-1})
Yearly average over 6 y (9 stations)	0.01	0.00	0.01	0.00	0.03	0.38*	0.19	0.00	0.00	0.02	0.00	0.05
Yearly average over 4 y (12 stations)	0.00	0.04	0.05	0.02	0.00	0.00	0.18	0.03	0.01	0.05	0.22	0.00
Yearly average over 2 y (16 stations)	0.17	0.00	0.13	0.07	0.02	0.31**	0.24*	0.13	0.09	0.03	0.03	0.43***

***Significant at 0.01 level; **significant at 0.05 level; *significant at 0.1 level; all other coefficients are not significant; A_{local}, local slope aspect; A_{valley}, general aspect of the main valley; LIM_1, distance to centre of nearest contiguous limestone area of 1 km^2; LIM_5, distance to centre of nearest contiguous limestone area of 5 km^2; S_{50up}, slope gradient over a vertical interval of 50 m upslope from the rain gauge; $S_{200down}$, slope gradient over a vertical interval of 200 m downslope from the rain gauge; $S_{500down}$, slope gradient over a vertical interval of 500 m downslope from the rain gauge.
[a] Using Eq. (5).

assessed in different ways for the 16 rainfall stations (Table 4), but were individually and in general not significant in explaining rainfall variability, neither at a scale of 40 km^2 (nine rain gauges), nor at a scale of 80 km^2 (16 gauges).

Given that slope aspect can take all trigonometrical directions, the relationship of local slope aspect or orientation of the valley to rain depth was expected to be best represented by a waveform function expressed by the model

$$P_{ann} = p_1 + p_2(\sin(a - p_3)) \quad (5)$$

where

P_{ann} expected mean annual precipitation (in mm)
a local or valley slope aspect (in deg, turning right from the N)

The three parameters are standing for

p_1 expected average annual rain depth (mm)
p_2 amplitude of the sinusoidal function (mm)
p_3 aspect (in deg) where average rain is expected.

A preliminary analysis with average rainfall of 4 y (Vandenreyken et al., 2001) showed a tendency where the largest rain depth is received by those stations oriented to the SE. The 'best fit' of Eq. (5) for the nine-stations dataset (average over 6 y) was however not very significant ($r^2 = 0.38$; $P < 0.1$) and in fact not totally representative since the dataset covered only 220°.

In order to obtain a dataset covering the whole range of slope aspects, and also to find possible explanatary factors of yearly rainfall variability in a wider area, the rain gauge network was gradually expanded to 16 stations.

This upscaling of the network (though with shorter time series) did not confirm the previous analysis. For a wider area, including 12 rain gauges, but only 4 y of data, not one single variable is significantly correlated with mean annual rain depth (Table 4). The multiple regression analysis yields a model with A_{local} and A_{valley}, in addition to Y, X' and Y'; determination coefficient is 0.53 and most of the variables are individually significant at level 0.001, except one at level 0.1.

At subregional scale (16 rain gauges with a 2 y' data series only), when elaborating the multiple regression model, the locational variables (X, Y, X' and Y') had to be removed first and finally the best model, with one variable significant at level 0.01, the two others at 0.001, was

$$P_{ann} = 2760 - 0.98z - 159\sin(A_{valley} - 122)) + 1746\, S_{500down} \quad (r^2 = 0.84,\ P < 0.001) \quad (6)$$

where

P_{ann} expected average yearly precipitation (in mm)
A_{valley} valley orientation (in deg, turning right from the N)
$S_{500down}$ average slope gradient (m m^{-1}) between the station and the nearest point with an elevation of 500 m less
z elevation (m a.s.l.)

As can be observed throughout this study, we found no evidence, at the scale of the study area, of significant rainfall increase with elevation. Eq. (6) shows even a negative impact of elevation. The most overriding factors are other topographical factors and especially slope aspect, general orientation of the valley and slope gradient over longer distances.

Variation in topography results in differences in yearly rain depth of 80 mm (average over 6 y) to more than 400 mm (average over 2 y). These observations are important for geomorphic processes and for agriculture, since those parts of the study area that are oriented to South and East and in the neighbourhood of important topographic height differences (cliffs) have better agricultural productivity or forest growth (Aerts et al., 2004), but are also more subject to erosion and landslide risk (Nyssen et al., 2002). However, an analysis of the importance of spatial rain variability (Vandenreyken, 2001) shows that it is second to other variables (lithology, slope gradient, vegetation cover) in explaining the spatial variability of soil erosion, runoff generation and landslide risk.

3.3. Rain intensity

Based on data recorded by the tipping bucket rain gauge, it was found that the intensity during events is quite variable. Low intensity storms show a more regular pattern. Generally, rain intensity is low during most of a storm and high during a small part of it; this high intensity period can be situated at the beginning, in the middle or at the end of the storm. The results obtained in this study do not confirm that peaks in Ethiopia are generally in the middle of storms, as measured by Krauer (1988).

Overall, rain intensity is not very high (Fig. 7a). Eighty eight percent of total rain volume falls with an intensity <30 mm h^{-1}. This contrasts strongly with the 77% rain with intensity >25 mm h^{-1} found by Hunting (1976) in Ilala, in a more arid environment, 40 km E of the study area, during one rainy season.

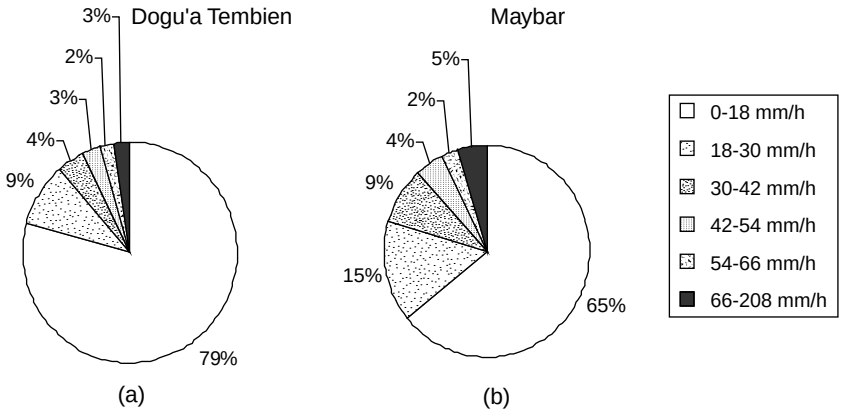

Fig. 7. Proportion of rain corresponding to different intensities. (a) Dogu'a Tembien (1998–2000) (this study); (b) Maybar/Wollo (1991–1994) (SCRP, 2000, MAPLREall.XLS database).

Table 5
Maximum recorded rain depth in the study area (1998–2000) for different time spans, compared to thresholds for excessive rain, as defined by Greer (1971)

Time span	Max. rain depth (mm)	Corresponding maximum rain intensity (mm h^{-1})	Threshold values for excessive rain (mm h^{-1})
1 min	2.4	144	
5 min	8.8	106	76
10 min	14.2	85	36
30 min	25	50	25
1 h	32.2	32	20
3 h	33.6	11	
6 h	33.6	6	
12 h	34	3	
24 h	34.2	1	

The validity of our data can however be accepted, taking into account (a) the longer observation period, (b) the fact that SCRP (2000) data in Wollo have a similar distribution (Fig. 7b), and (c) our own observations during long stays (6 y) in the study area.

From the tipping bucket rain gauge data, maximum rain depths (during 1998–2000) for given time spans were calculated (Table 5) and compared to values defined by Greer (1971) as excessive. Rain intensities beyond these thresholds caused >50% of total soil loss on runoff plots of the Soil Conservation Research Project (SCRP) (Krauer, 1988).

A stabilisation in maximum rain depth takes place at the 1-h time span, indicating that high intensities do not last long. It should however be noted that these maxima exceed by far the threshold values for excessive rain. These maxima are highest in the rainy season, but, unlike total rain, there is no marked peak: e.g. maximum rain depth during 1 min is 2–2.4 mm for each month, from June to September. Even exceptional rains during the dry season can be very intensive.

3.4. Raindrop size and rain intensity

Measured drops were classified according to their size and to rain intensity (Table 6). For each intensity, the D_{50} or median volume drop diameter was determined, i.e. half of the rain volume falls in drops smaller than the D_{50} and half in larger drops. Theoretically, some 10,000 drops should be sampled for every intensity class to have a D_{50} with low standard deviation (Salles et al., 1999). This could not be realised due to time constraints, hence the large standard deviations for some classes (Table 6). For the intensities of 1.09 and 96 mm h^{-1}, only less than 200 drops could be registered; these intensities have been left out from the analysis.

Table 6
Median volume drop diameter (D_{50}) for each rain intensity

Intensity (mm h^{-1})	Number of drops	D_{50} (mm)	St. dev. (mm)
0.57	860	1.5	0.5
0.8	613	1.2	0.3
1	674	2.2	1.4
1.09[a]	175	3.7	7.8
1.33	2989	2.1	1.2
1.5	1928	2.5	2.0
1.71	5069	1.9	0.8
2	1950	2.1	1.2
2.4	3766	2.5	1.9
3	6944	2.5	2.0
4	8783	2.1	1.0
6	6899	2.3	1.4
12	5980	3.1	3.5
24	4955	4.0	7.3
36	3529	4.1	8.3
48	2240	3.7	6.4
60	1362	4.0	7.5
72	586	4.4	9.8
84	661	3.8	6.2
96[a]	107	3.0	3.3

[a] The number of raindrops recorded was insufficient, hence these intensities were not used in the analysis.

The relation between D_{50} and rain intensity (Fig. 8), unlike the often found power model (Eq. (1)), can in our study area best be represented

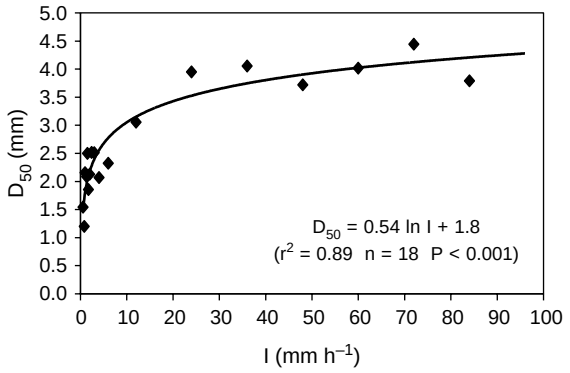

Fig. 8. Median volume drop diameter (D_{50}) vs. rain intensity (I).

by a logarithmic regression (Vandenreyken, 2001)

$$D_{50} = 0.54 \ln(I) + 1.8 \quad (r^2 = 0.89;\ n = 18;\ P < 0.001) \tag{7}$$

where

D_{50} median volume drop diameter (mm)
I rain intensity (mm h^{-1})

Kurtosis of drop-size distributions, representing rain volume as a function of drop size, is more peaked for low intensities and less for larger intensities, indicating a larger drop size variability (Fig. 9). For each rain intensity, median volume drop diameters are larger than those observed elsewhere, e.g. in Zimbabwe (Hudson, 1971), or Hong-Kong (Jayawardena and Rezaur, 2000), or in the theoretical Marshall–Palmer model (Brandt, 1990). As stated before, intensities <12 mm h^{-1} were measured over periods >1 min. Furthermore, other studies (e.g. Jayawardena and Rezaur, 2000) also used 1 min intervals to measure rain intensity. Hence, observed differences cannot be ascribed to differences in intensity measurement methods.

The larger rain drop sizes in our study area can be explained by the nature of rain distribution and by elevation. It has been shown that in continental semi-arid to subhumid areas, storms with relatively high energy contents are frequent (Van Dijk et al., 2002). In such areas, part of the precipitation falls as (melted) hail. This is also the case in the study area. Furthermore, the high elevation of the study area leads to decreased fall height. Therefore less evaporation takes place while the drops travel through under-saturated air before reaching the soil surface; due to shorter fall duration, the chance of disintegration due to turbulence (Hudson, 1971; Maidment, 1993) is also decreased. Our results seem thus to contradict the results of the only known previous study including mountain areas (up to 2250 m a.s.l. in Hawaii; Blanchard, 1953), where 'apparently smaller' raindrops were found at high altitudes.

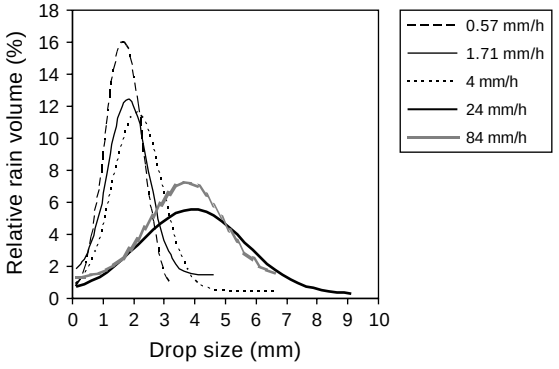

Fig. 9. Relative rain volume per drop size for different rain intensities.

3.5. Rain kinetic energy

For each rain intensity, the kinetic energy per drop size class was determined using Eq. (2). The different classes were then summed to obtain the total volume-specific kinetic energy (in J m^{-2} mm^{-1}), which was converted into time-specific kinetic energy, expressed in J m^{-2} h^{-1}. As observed by Salles et al. (2002), also in our data set, the linear regression of Ek_{time} on rain intensity I

$$Ek_{time} = 36.65\, I - 22.1 \quad (r^2 = 0.99;\ n = 18) \tag{8}$$

yields a better correlation than the logarithmic regression of Ek_{vol} on I (Fig. 10):

$$Ek_{vol} = 3.45 \ln I + 22.9 \quad (r^2 = 0.82;\ n = 18) \tag{9}$$

A regression of the 'classic' Ek_{vol} on rain intensity can be made either by the commonly used logarithmic regression (Eq. (9)), or by re-arranging the regression equation for Ek_{time} (Eq. (8)):

$$Ek_{time}/I = (36.65\, I - 22.1)/I, \tag{10}$$

or

$$Ek_{vol} = 36.65(1 - (0.6/I)) \quad (I \geq 0.6 \text{ mm } h^{-1}) \quad (r^2 = 0.99, n = 18) \quad \text{(Vandenreyken, 2001)} \tag{11}$$

Eq. (11) describes nearly perfectly the relation between kinetic energy and rain intensity in the study area (Fig. 10). It is however very different from relations found elsewhere: intensities smaller than 70 mm h^{-1} have a larger kinetic energy. This is especially due to the large D_{50} for these intensities. Furthermore, the adoption of a model of the type $Ek_{vol} = a\ (1 - b/I)$ allows a better representation of kinetic energy for lower intensities. However, from a physical standpoint, any value of $I > 0$ must have

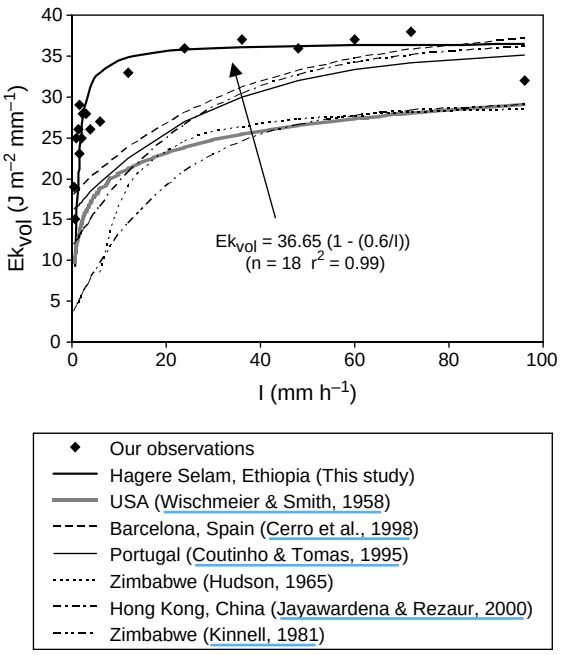

Fig. 10. Equations representing volume-specific kinetic energy (Ek_{vol}) vs. rain intensity (I).

a value of $Ek_{vol} > 0$ so that (Eq. (11)) is a pragmatic approximation that is not valid at very low rainfall intensities. Noteworthy is also the stabilisation of kinetic energy for intensities >20 mm h^{-1}.

Eq. (11) has important implications for the calculation of the rain erosivity factor R of the (Revised) Universal Soil Loss Equation ((R)USLE):

$$R = \sum(EI_{30})/N \quad (12)$$

(Renard et al., 1997) where

E total storm energy
I_{30} maximum 30-min intensity
N period of observation (y).

Since the direct measurement of E is difficult, it is often computed from rain intensity data collected by pluviograph (e.g. for Ethiopia by Krauer (1988)), using

$$E = 11.87 + 8.73 \log_{10} I \quad (13)$$

(Wischmeier and Smith, 1958) or

$$E = 29(1 - 0.27 \exp(-0.05I)) \quad (14)$$

(Brown and Foster, 1987; Renard et al., 1997) an equation that yields results which are similar to those obtained when using Kinell's (1981) equation.

These relations, represented in Fig. 10, however give values for Ek_{vol} that are significantly smaller than values observed in the study area. Hence, R will also be underestimated. Based on the present study, which includes the only raindrop size measurement ever carried out in Ethiopia, we would recommend to use Eq. (11), rather than (13) or (14) in calculations of the rain erosivity factor (R) for stations in the Ethiopian Highlands. Given the fact that there are great standard deviations on median volume drop diameter at most intensities (see Table 6), a high scatter in Eq. (11) can be expected when using short-term data; hence this equation is only destined to be used in calculations of yearly R values.

4. Conclusions

Despite the short observation period (6 y, and some stations only 2 or 4 y), several conclusions can be drawn. In the 80-km^2 study area, topographical aspects such as steep overall slope gradients (expressed by the presence of important cliffs), valley aspect, but not elevation, control the spatial distribution of annual rain depth. A non-linear multiple regression model (Eq. (6)), represents this rainfall distribution. Rain depth is highest in those places where air masses flowing through preferred flow paths (large valleys) are lifted over important differences in elevation. Next to factors related to the land and its cover, differences of more than 200 mm yearly rain can have important repercussions on erosion processes, agricultural productivity, and sometimes on waterlogging.

Besides the daily variability, with more than half of the rain volume in the afternoon, temporal variability throughout the year is especially important. The period October–April is nearly dry; July and August take the largest share in yearly rain.

Rain intensity is lower than expected: 88% falls with an intensity <30 mm h^{-1}. High intensities have a short duration; maximum rain depth over 1 h is nearly the same as the one over 24 h.

For all rain intensities, the median volume drop diameters (D_{50}) are larger than those found in other regions, probably due to the nature of the climate

(semi-arid to subhumid mountain climate). Large rain erosivity is due to large drop sizes, rather than to high rain intensities.

A new relation between rain intensity and kinetic energy was developed (11). Due to large drop sizes, it yields, within the range [0.6–84 mm h^{-1}], larger values for Ek_{vol} than elsewhere in the world. It is suggested to use this relationship (11) for calculating average Ek_{vol} values in the Ethiopian Highlands, and for the computation of the yearly (R)USLE's rain erosivity factor.

Acknowledgements

This study is part of research programme G006598 funded by the Fund for Scientific Research—Flanders, Belgium. Financial support by the Flemish Interuniversity council (VLIR, Belgium) is acknowledged. Thanks go to Berhanu Gebremedhin Abay for continuous field assistance and monitoring of the rain gauge network. Numerous farmers, the local Agricultural Office, REST (Relief Society of Tigray) branch and the authorities of the concerned villages and district facilitated the research. Many thanks go to all people who faced the difficult *kramat* rainy seasons with us, and especially the secondary school students who read the rain gauges daily as well as our fellow rain drop outliners. Constructive comments by Donald McCool and an anonymous reviewer are gratefully acknowledged.

References

Abebe Yeshanew, Apparao, G., 1989. Annual rain water potential and its variability in drought years over Ethiopia, in: Conference on Climate and Water, Helsinki, Finland, September 1989, vol. 1. Suomen Akatemian [Helsinki], pp. 219–235.

Aerts, R., Wagendorp, T., November, E., Mintesinot Behailu, Deckers, J., Muys, B., 2004. Ecosystem thermal buffer capacity as an indicator of the restoration status of protected areas in the Northern Ethiopian highlands. Restor. Ecol. 12 (4), 586–596.

Aina, P.O., Lal, R., Taylor, G.S., 1977. Soil and crop management in relation to soil erosion in the rainforest of Western Nigeria, in: Foster, G.R. (Ed.), Soil Erosion: Prediction and Control. Soil Conservation Society of America, Ankeny, pp. 75–82.

Arkin, Y., Beyth, M., Dow, D.B., Levitte, D., Temesgen Haile, Tsegauge Hailu, 1971. Geological Map of Mekele Sheet Area ND 37-11, Tigre Province, 1:250.000. Imperial Ethiopian Government, Ministry of Mines, Geological Survey, Addis Ababa.

Beguin, H., 1979. Méthodes d'analyse géographique quantitative. Librairies Techniques, Paris, p. 283.

Beyth, M., 1972. Paleozoic–Mesozoic sedimentary basin of Makalle outlier. Am. Assoc. Pet. Geologists Bull. 56, 2426–2439.

Blanchard, D.C., 1953. Raindrop size distributions in Hawaiian rains. J. Meteorol. 10, 457–473.

Brandt, C.J., 1990. Simulation of the size distribution and erosivity of raindrops and throughfall drops. Earth Surf. Process. Landforms 15, 687–698.

Brown, L., Foster, G., 1987. Storm erosivity using idealised intensity distribution. Trans. ASAE 30, 379–386.

Camberlin, P., 1994. Les précipitations dans la Corne orientale de l'Afrique: climatologie, variabilité et connexions avec quelques indicateurs océano–atmosphériques. PhD dissertation, Université de Bourgogne, p. 379.

Cerro, C., Bech, J., Codina, B., Lorente, J., 1998. Modeling rain erosivity using distrometric techniques. Soil Sci. Soc. Am. J. 62 (3), 731–735.

Conway, D., 2000. Some aspects of climate variability in the North East Ethiopian Highlands—Wollo and Tigray. Sinet: Ethiop. J. Sci. 23 (2), 139–161.

Coutinho, M., Tomas, P., 1995. Characterization of raindrop size distributions at the Vale Formoso Experimental Erosion Centre. Catena 25 (1–4), 187–197.

Daniel Gamachu, 1977. Aspects of climate and water budget in Ethiopia. Addis Ababa University Press, p. 71.

Eklundh, L., Pilesjö, P., 1990. Regionalization and spatial estimation of Ethiopian mean annual rainfall. Int. J. Climatol. 10, 473–494.

Ethiopian Mapping Authority, 1996. Ethiopia 1:50000, Series ETH 4, Sheets 1339 A3 (Abiy Adi) and A4 (North Mekele), Addis Ababa.

Garland, C., 1980. Geology of the Adigrat Area, Ministry of Mines, Energy and Water Resources. Geological Survey of Ethiopia, Addis Ababa, p. 51.

Goebel, W., Odenyo, V., 1984. Ethiopia. Agroclimatic resources inventory for land-use planning. Ministry of Agriculture, Land Use Planning and Regulatory Department, UNDP, FAO. Technical Report DP/ETH/78/003, vol. 1, p. 208; vol. 2, p. 95.

Greer, J., 1971. Effect of excessive-rate rainstorms on erosion. J. Soil Water Conserv. 5, 196–197.

Griffiths, J.F., 1978. Applied Climatology—An Introduction. Oxford University Press, Oxford, p. 136.

Hall, M., 1970. Use of the stain method in determining the drop size distribution of coarse liquid sprays. Trans. Am. Soc. Agric. Eng. 13, 33–37.

Hemming, C.F., 1961. The ecology of the coastal area of Northern Eritrea. J. Ecol. 49, 55–78.

Houghton, D.D., 1985. Handbook of Applied Meteorology. Wiley, New York, p. 1461.

Hudson, N., 1965. The influence of rainfall mechanics on soil erosion. MSc Thesis, Cape Town.

Hudson, N., 1971. Soil Conservation. Billing & Sons Ltd, Great Britain, p. 320.

Hulme, M., 1990. Rainfall changes in Africa: 1931–1960 to 1961–1990. Int. J. Climatol. 12, 685–699.

Hunting, T.S., 1976. Tigrai Rural Development Study, Annex 2: Water Resources, vol. 1: Hydrology and Surface Water. Hunting Technical Services Ltd, Hemel Hempstead, GB, p. 213.

Hutchinson, R.W., Engels, G.G., 1970. Tectonic significance of regional geology and evaporite lithofacies in northeastern Ethiopia. Phil. Trans. R. Soc. Lond. A. Math. Phys. Sci. 267, 313–330.

Jayawardena, A.W., Rezaur, R.B., 2000. Drop size distribution and kinetic energy load of rainstorms in Hong Kong. Hydrol. Process. 14, 1069–1082.

Kinnell, P., 1981. Rainfall intensity kinetic-energy relationships for soil loss prediction. Soil Sci. Soc. Am. J. 45 (1), 153–155.

Kowal, J.M., Kassam, A.H., 1976. Energy and instruments intensity of rainstorms at Samary, northern Nigeria. Trop. Agric. 53, 185–198.

Krauer, J., 1988. Rainfall, erosivity and isoerodent map of Ethiopia. Soil Conservation Research Project, Research Report 15. University of Berne, Switzerland, p. 132.

Lal, R., 1998. Drop size distribution and energy load of rainstorms at Ibadan, Western Nigeria. Soil Tillage Res. 48, 103–114.

Laws, J., 1941. Measurements of the fall-velocity of water-drops and raindrops. Hydrology 22, 709–721.

Maidment, D.R., 1993. Handbook of Hydrology. McGraw-Hill, Inc., New York.

Marquinez, J., Lastra, J., Garcia, P., 2003. Estimation models for precipitation in mountainous regions: the use of GIS and multivariate analysis. J. Hydrol. 270 (1–2), 1–11.

Mattson, J., Rapp, A., 1991. The recent droughts in western Ethiopia and Sudan in a climatic context. Ambio 20 (5), 172–175.

Merla, G., Abbate, E., Azzaroli, A., Bruni, P., Canuti, P., Fazzuoli, M., Sagri, M., Tacconi, P., 1973. A Geological Map of Ethiopia and Somalia (1973) 1:2.000.000 and Comment. University of Florence, Italy.

Messerli, B., Rognon, P., 1980. The Saharan and East African uplands during the quaternary, in: Williams, M., Faure, H. (Eds.), The Sahara and the Nile. Quaternary Environments and Prehistoric Occupation in Northern Africa. Balkema, Rotterdam, pp. 87–132.

Mohr, P., 1963. The Geology of Ethiopia. University College of Addis Ababa Press, p. 270.

Moore, T.R., 1979. Rainfall erosivity in East Africa. Geografiska Annaler 61A, 147–156.

Nyssen, J., Mitiku Haile, Moeyersons, J., Poesen, J., Deckers, J., 2000. Soil and water conservation in Tigray (Northern Ethiopia): the traditional daget technique and its integration with introduced techniques. Land Degrad. Dev. 11 (3), 199–208.

Nyssen, J., Moeyersons, J., Poesen, J., Deckers, J., Mitiku Haile, 2002. The environmental significance of the remobilisation of ancient mass movements in the Atbara-Tekeze headwaters, Northern Ethiopia. Geomorphology 49, 303–322.

Nyssen, J., Poesen, J., Moeyersons, J., Deckers, J., Mitiku Haile, Lang, A., 2004. Human impact on the environment in the Ethiopian and Eritrean Highlands—a state of the art. Earth Sci. Rev. 64 (3–4), 273–320.

Obi, M.E., Salako, F.K., 1995. Rainfall parameters influencing erosivity in southeastern Nigeria. Catena 24, 275–287.

Poesen, J., 1983. Regenerosiemechanismen en bodemerosiegevoeligheid. PhD Thesis, Katholieke Universiteit Leuven, Department Geography—Geology.

Renard, K.G., Foster, G.R., Weesies, G.A., McCool, D.K., Yoder, D.C., et al., 1997. Predicting soil erosion by water: a guide to conservation planning with the Revised Universal Soil Loss Equation (RUSLE). Agriculture Handbook 703. United States Department of Agriculture, Washington, p. 404.

Rudloff, W., 1981,. World climates, Stuttgart, Wissenschaftliche Verlagsgesellschaft 1981, p. 632.

Salles, C., Poesen, J., 1999. Performance of an optical spectro pluviometer in measuring basic rain erosivity characteristics. J. Hydrol. 218, 142–156.

Salles, C., Poesen, J., Borselli, L., 1999. Measurement of simulated drop size distribution with an optical spectro pluviometer: sample size considerations. Earth Surf. Process. Landforms 24, 545–556.

Salles, C., Poesen, J., Sempere-Torres, D., 2002. Kinetic energy of rain and its functional relationship with intensity. J. Hydrol. 257 (1–4), 256–270.

SCRP, 2000. Area of Maybar, Wello, Ethiopia: Long-term Monitoring of the Agricultural Environment 1981–1994. Soil Erosion and Conservation Database. Soil Conservation Research Project, Berne and Addis Ababa, p. 81.

Suzuki, H., 1967. Some aspects of Ethiopian climates. Ethiop. Geographical J. 5 (2), 19–22.

Troll, C., 1970. Die naturräumliche Gliederung Eritreas. Erdkunde 24 (4), 249–268.

Vandenreyken, H., 2001. Ruimtelijke en temporele variaties van neerslag en zijn erosiviteit in een tropisch berggebied, Noord-Ethiopië. Unpub. MSc Thesis. Department of Geography, K.U. Leuven, p. 310.

Vandenreyken, H., Poesen, J., Moeyersons, J., Nyssen, J., 2001. Ruimtelijke en temporele variaties van neerslag en zijn erosiviteit in een tropisch berggebied in Noord-Ethiopië. De Aardrijkskunde 25 (4), 13–24.

Van Dijk, A., Bruijnzeel, L., Rosewell, C., 2002. Rainfall intensity—kinetic energy relationships: a critical literature appraisal. J. Hydrol. 261, 1–23.

Wischmeier, W., Smith, D., 1958. Rainfall energy and its relationship to soil loss. Trans. AGU 39, 285–291.

Yilma Seleshi, Demarée, G., 1995. Rainfall variability in the Ethiopian and Eritrean highlands and its links with the Southern Oscillation Index. J. Biogeography 22, 945–952.